Steady State Jet Impingement Heat Transfer from Conical Shaped Wall Geometry

Arpit Dwivedi
Department of Mechanical Engineering
Indian Institute of Technology, Bombay
Mumbai, India
200100032@iitb.ac.in

Abstract

The report presents the Numerical computations performed in ANSYS Fluent over a cylindrical jet impinged over a conical plate to analyze the cooling effect of jet impingement. The jet flow is in the range of complete turbulent flow. The computational results were obtained for different cases by varying geometrical parameters like the nozzle-to-plate spacing($z = H$) ratio to the nozzle diameter(D), the included angle of cone(ϕ), Offset ratio of pipe position from the axis of cone(O/D). Taking one step further computations have been performed for a case by replacing the conical vertex with a hemispherical end. The radius of the hemishpere has also been changed to observe the shift in peak of surface Nusselt number along the wall surface.The in-house experimental data of surface Nusselt number for different cases has been used for validating the Nusselt number obtained from computations.

I. Introduction

Impinging jets on walls have very high heat transfer performances hence these configurations are widely used in the industrial realm where a high-performance heat transfer configuration is needed. The configuration can be varied a lot by varying geometrical parameters such as H/D, number of jets, the geometrical arrangement of jets and shape of wall. The paper focus on the case when we use a conical shape wall onto which jet is impinged. The efficiency and feasibility are checked before using the configuration in the desired situation in Industries. The application of jet impingement is broadly separated into two categories: heating/cooling configurations either at a constant wall temperature (quench cooling) or at a uniform wall heat flux (electronic components cooling).

The current paper discusses the jet impingement over a conical shaped wall. Analytically obtaining solutions for such cases is difficult and we have performed numerical computations on ANSYS for different cases and the obtained results are compared with the in-house experimental data. Unlike the case of Flat plate jet impingement where the peak in Nusselt number occurs at centre, in the conical wall plate the peak has shifted away from the centre. The Nusselt numbers near the apex are very less and peak is observed after a certain distance from the vertex. The vertex had been blended and replaced with hemispherical shaped cup to observe the changes in surface Nusselt number and how the peak shifts on replacing the sharp end. Lastly the pipe has been given an offset distance from the axis to observe how the values would change by varying this parameter(O/D).

A. *Uniform wall heat flux*

Under uniform wall heat flux(q) condition radial distribution of temperature($T(r)$) for fluid just above the wall is obtained from ANSYS computational results. Now as

$$q = h(T(r) - T_j) \tag{1}$$

$$h(r) = \frac{q}{T(r) - T_j} \tag{2}$$

The local convective heat transfer coefficient($h(r)$) is calculated from the Temperature field($T(r)$).Now as

$$Nu = \frac{h.D}{k} \tag{3}$$

Therefore, local Nusselt number can be calculated from:

$$Nu(r) = \frac{h(r).D}{k} \tag{4}$$

The Surface Nusselt number is directly provided by ANSYS computational results.

B. *Constant wall temperature*

Under constant wall temperature(T_w) condition, radial distribution of temperature gradient, normal to the wall is calculated and since

$$q = -k\frac{\partial T}{\partial z} \tag{5}$$

the term $\frac{\partial T}{\partial z}$ is approximated to $\frac{\Delta T}{\Delta z}$ where ΔT is calculated by obtaining the difference in Temperature at two nodes separated by Δz normal to the wall. Then again obtaining the radial distribution of temperature($T(r)$) for fluid just above the wall and using (1), (2) and (4) local Nusselt number is obtained.
The Surface Nusselt number is directly provided by ANSYS computational results. .

II. CASE I :: ZERO ECCENTRICITY

*1) **Geometrical Setup**:* The geometrical arrangement involves a conical wall surface with cylindrical pipe out of which jet comes out with concentric axes[Fig XX]. The included angle of cone are 30°and 70°as two cases for computations. The impinging jet is in turbulent realm with Reynolds number of 29,000.
For included angle 30°: The diameter of pipe was chosen to be 2 cm and the length of pipe(L_1 = 12.5 cm).i.e..L_1/D = 6.25. The nozzle is at a distance of 8.5 cm above the apex.i.e..L/D = 4.25.
For included angle 70°: The diameter of pipe was chosen to be 2 cm and the length of pipe(L_1 = 8 cm).i.e..L_1/D = 4. The nozzle is at a distance of 6 cm above the apex.i.e..L/D = 3.

*2) **Mesh**:* Different types of mesh with different inflation layers near the wall and element size of wall face have been used for computation for both the cases of included angles. The smoothness level of each mesh has been set to medium and the tetrahedral mapped mesh type is used for computations. The element behaviour has been chosen Quadratic for computations which has significantly good accuracy as online literature told regarding accuracy. While meshing we need to refine mesh near wall so that we can increase the number of nodes there for results with better accuracy. In the different types of grids used, the parameters were maneuvered to increase the number of nodes near wall and keeping y^+ nearly 1.

*3) **Computational Setup and Results**:* The computations were done using steady-state, Pressure based(in-compressible fluid) and absolute velocity formulation type solver.The model used was $k-\omega$ SST as the results are accurate in predicting boundary layer with adverse pressure gradient and therefore the results from it are near the experimental values. The convergence criteria used for all the parameters were 10^{-3} except for energy which had 10^{-6}. The simulation had been stopped when the residual plot during simulation do not show further decline, their order began to fluctuate with little amplitude of order $10^{-4} or 10^{-5}$ or nearly become constant. In general all other parameters velocity, energy, , ω satisfy or achieve the convergence criteria except continuity. The iteration for the simulations have been increased to observe the change but the continuity didn't reached below the order of convergence criteria in some cases. The computations had been stopped when the residuals reached the order of these criteria.

- **(A)** $\phi = 30, Re = 29,000, L_1/D = 6.25 \& L/D = 4.25$ **::**

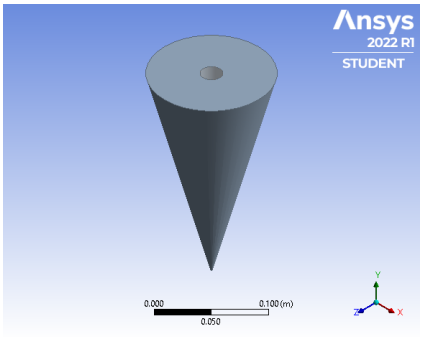

(a) Geometry for $\phi = 30, L_1/D = 6.25 \& L/D = 4.25$

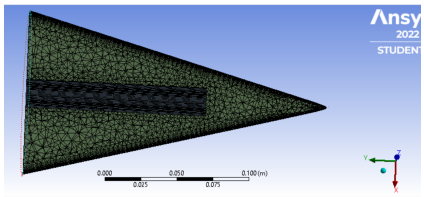

(b) Mesh for $\phi = 30, L_1/D = 6.25 \& L/D = 4.25$

Fig. 1: Experimental Data vs Computational data for Surface Nusselt Number

The geometrical setup is shown in figure above. The boundary topmost inner circular portion is free stream inlet of flow. The wall had uniform heat flux of $6000 W/m^2$. The inlet temperature of free stream is 300 K. The outlet condition is kept as Pressure outlet as in our problem whole configuration is enclosed by atmospheric pressure.

The meshing has been done to set greater nodes near wall compared to other regions. The figure above shows the same. The table below contains information about the parameters that had been varied to obtain the grid insensitive results. The student license has a limit of 512000 elements hence i had to stop after achieving a number near the threshold value.

Grid_ID	Inflation Layers	Face Sizing(m)	Number of Nodes	Number of Elements	Element Behaviour
Grid-1	30	0.005	943188	303127	Quadratic
Grid-2	30	0.0034	1312033	458379	Quadratic

TABLE I: Grid Info

Computational Results:
The surface Nusselt Number along conical wall plate at different angles had been computed from ANSYS for all cases(see fig below). The grid 2 results had been chosen for comparison with experimental data provided. The plot below shows the comparison between experimental and computational results. The convergence criteria used for all the parameters were 10^{-3} except for energy which had 10^{-6}. The computations had been stopped when the residuals reached the order of these criteria.

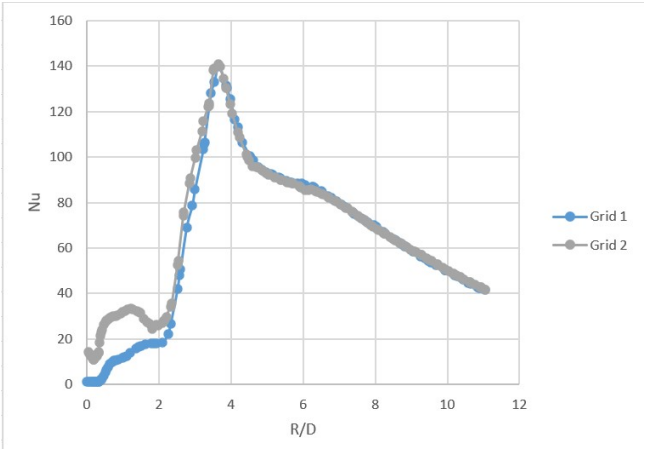

(a) Grid 1 & 2 at $\theta = 0$

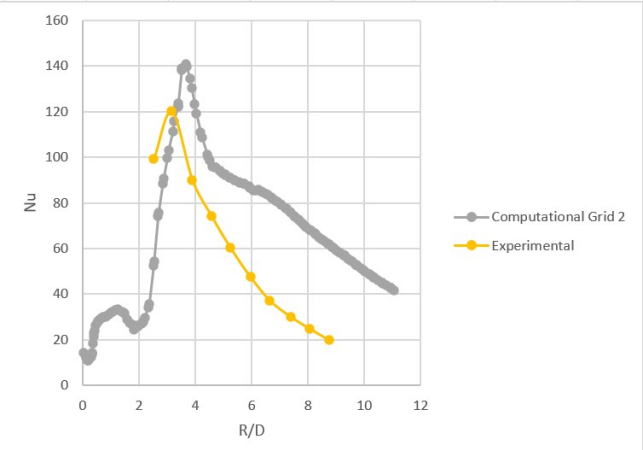

(b) Experimental Data vs Computational data at $\theta = 0$

Fig. 2: Nusselt Number Plots

Conclusions:

- The maximum variation in Nusslet number after R/D = 2.51 in plot between Grid 1 and Grid 2 is nearly 9%. Hence changing grid size further will not result in much significant change. We are interested in region after R/D = 2.51 as we have the experimental data in that region only due to experimental limitations.
- The deviation from the experimental value of the peak position(R/D) of Nusselt number is about 16.9% and for peak values of Nusselt number it is about 16.3%. The general trend in Nusselt number obtained computationally is similar to the trend observed from experimental data. The error in region $R/D > 5$ is much large almost 100% for some values.
- The velocity vector plot is shown below depicts how the flow pattern is over walls after jet crosses nozzle.

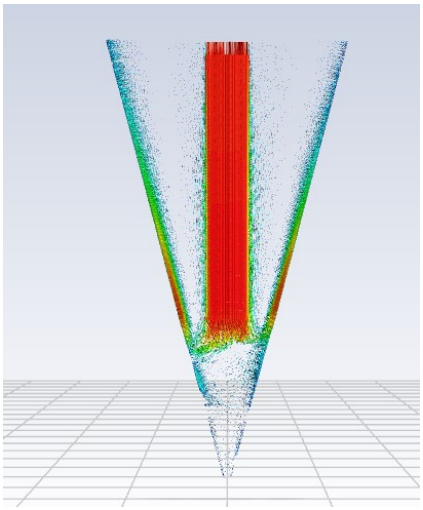

(a) Velocity Vectors

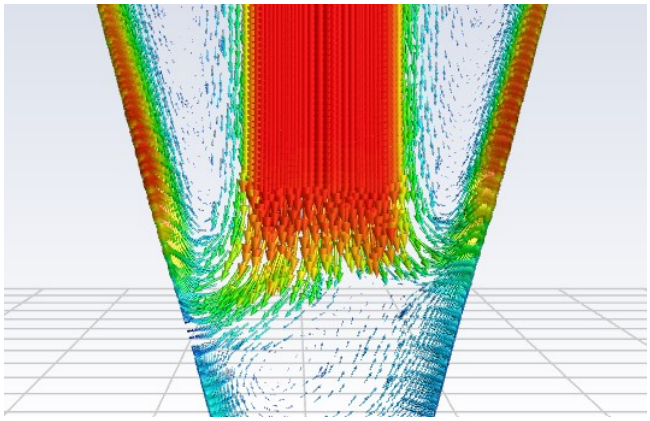

(b) Velocity Vectors Zoomed view

Fig. 3: Velocity Vectors

- The turbulence intensity and surface Nusselt number both have the maximum value around same region as we can see the contour attached below.
- The Pressure has a sharp declined as soon as it reaches the region of peak turbulence intensity. .

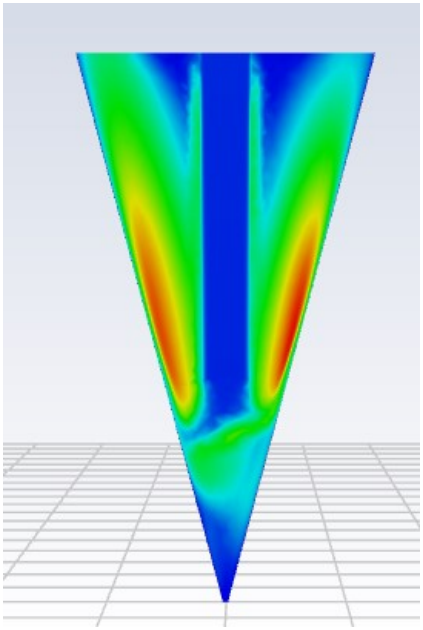

(a) Turbulence Intensity Contour

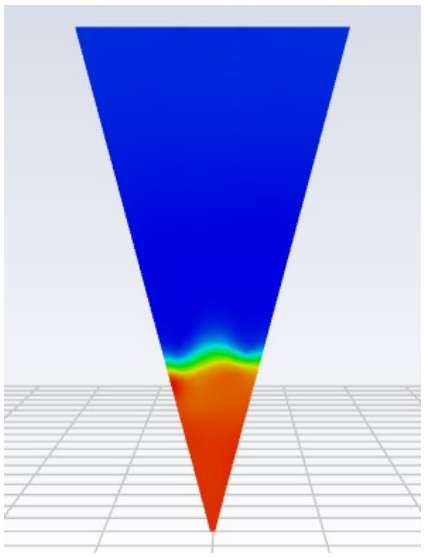

(b) Pressure Contour

Fig. 4: Contours

- **(B)** $\phi = 70, Re = 29,000, L_1/D = 4 \& L/D = 3$ **::**

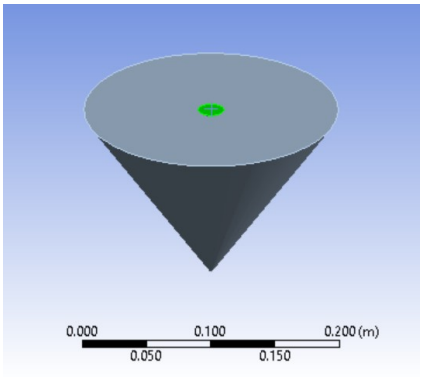

(a) Geometry for $\phi = 30, L_1/D = 4 \& L/D = 3$

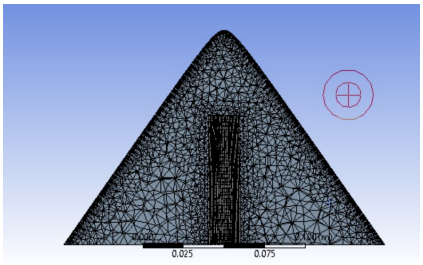

(b) Mesh for $\phi = 30, L_1/D = 4 \& L/D = 3$

Fig. 5: Experimental Data vs Computational data for Surface Nusselt Number

The geometrical setup is shown in figure above. The boundary topmost inner circular portion(marked green) is free stream inlet of flow. The wall had uniform heat flux of $6000W/m^2$. The inlet temperature of free stream is 300 K. The outlet condition is kept as Pressure outlet as in our problem whole configuration is enclosed by atmospheric pressure.

The meshing has been done to set greater nodes near wall compared to other regions. The figure above shows the same. The table below contains information about the parameters that had been varied to obtain the grid insensitive results.

Grid_ID	Inflation Layers	Face Sizing(m)	Number of Nodes	Number of Elements	Element Behaviour
Grid-1	30	0.005	846694	301549	Quadratic
Grid-2	30	0.004	1081693	401778	Quadratic
Grid-3	30	0.0034	1322444	505021	Quadratic

TABLE II: Grid Info

Computational Results:
The surface Nusselt Number along conical wall plate at different angles had been computed from ANSYS for all three cases(see fig below). The grid 3 results had been chosen for comparison with experimental data provided. The plot below shows the comparison between experimental and computational results. The convergence criteria used for all the parameters were 10^{-3} except for energy which had 10^{-6}. The computations had been stopped when the residuals reached the order of these criteria.

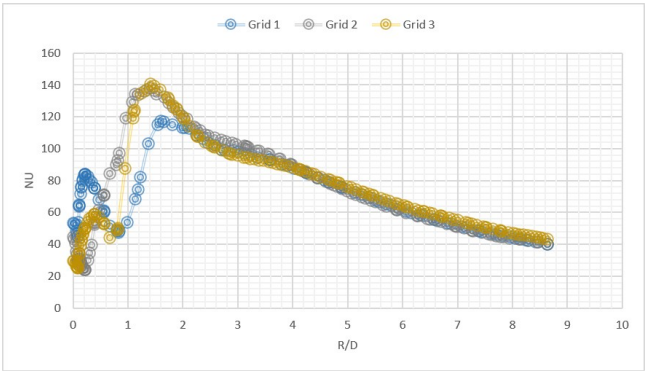

(a) Grid 1, 2 & 3 at $\theta = 0$

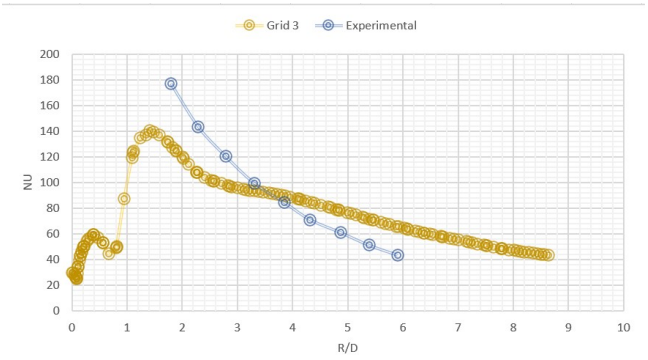

(b) Experimental Data vs Computational data at $\theta = 0$

Fig. 6: Nusselt Number Plots

Conclusions:

- The maximum variation in Nusslet number after R/D = 1 in plot between Grid 2 and Grid 3 is less than 5%. Hence changing grid size further will not result in much significant change in the interested region. We are interested in region after R/D = 1.5 as we have the experimental data in that region only due to experimental limitations.
- The experimental data had not clear value of peak Nusselt number due to limitations. However the predicted peak position by computations is at $R/D \approx 1.5$. The maximum error with the experimental data is 48% in the region $R/D > 5$.

– The velocity vector plot is shown below depicts how the flow pattern is over walls after jet crosses nozzle.

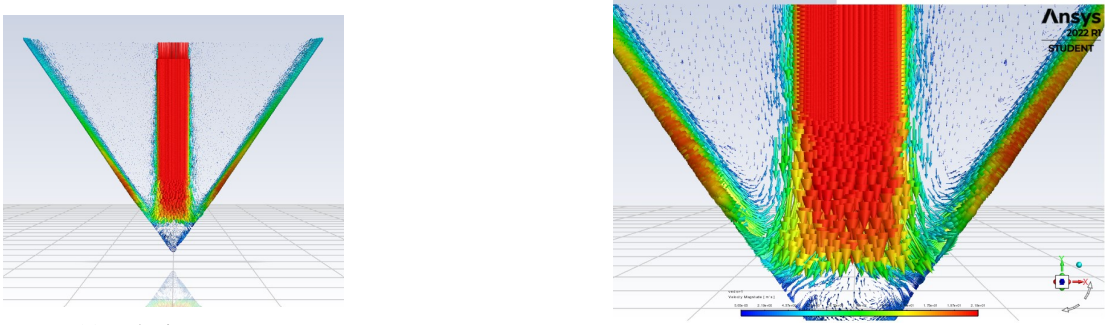

(a) Velocity Vectors

(b) Velocity Vectors Zoomed view

Fig. 7: Velocity Vectors

– The turbulence intensity and surface Nusselt number both have the maximum value around same region as we can see the contour attached below.
– The Pressure has a sharp declined as soon as it reaches the region of peak turbulence intensity.

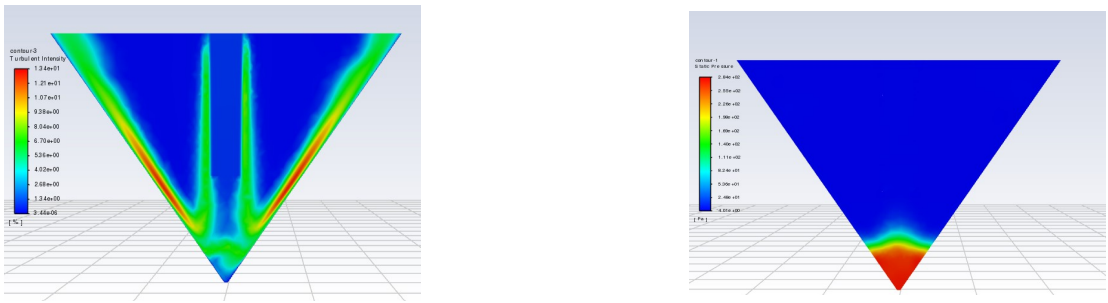

(a) Turbulence Intensity Contour

(b) Pressure Contour

Fig. 8: Contours

III. CASE II : NON-ZERO ECCENTRICITY

*1) **Geometrical Setup**:* The geometrical arrangement involves a conical wall surface with cylindrical pipe out of which jet comes out with eccentricity ratio of 0.5[Fig XX]. The included angle of cone are 30°and 70°as two cases for computations. The impinging jet is in turbulent realm with Reynolds number of 29,000 for 30°and 82,000 for 70°.

For included angle 30°: The diameter of pipe was chosen to be 2 cm and the length of pipe(L_1 = 12 cm for one case and 0 cm for the other case).i.e..L_1/D = 6 and 0 respectively. The nozzle is at a distance of 8.5 cm and 20.5 cm above the apex.i.e..L/D = 4.25 and 10.25.

For included angle 70°: The diameter of pipe was chosen to be 2 cm and the length of pipe(L_1 = 8 cm).i.e..L_1/D = 4. The nozzle is at a distance of 6 cm above the apex.i.e..L/D = 3.

*2) **Mesh**:* Different types of mesh with different inflation layers near the wall and impinging pipe and element size of wall face have been used for computation for both the cases of Included angles. The table above contains the information regarding the Grids. The smoothness level of each mesh has been set to medium and the tetrahedral mapped mesh type is used for computations. The element behaviour has been kept Quadratic for computations which has significantly greater number of nodes compared to linear in the geometry. While meshing we need to refine mesh near wall so that we can increase the number of nodes there for results with better accuracy. In the three different type of grids used, the parameters were maneuvered to increase the number of nodes near wall and keeping y^+ nearly 1.

*3) **Computational Setup and Results**:* The computations were done using steady-state, Pressure based(in-compressible fluid) and absolute velocity formulation type solver.The model used was $k-\omega$ SST. The convergence criteria used for all the parameters were 10^{-3} except for energy which had 10^{-6}. The computations had been stopped when the residuals reached the

order of these criteria

- **(A)** $\phi = 30, Re = 29,000, L_1/D = 6 \& L/D = 4.25$ **::**

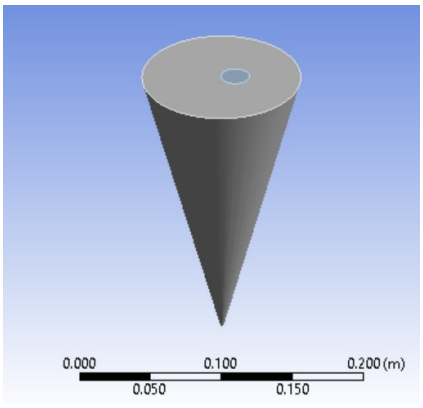

(a) Geometry for $\phi = 30, L_1/D = 6 \& L/D = 4.25$

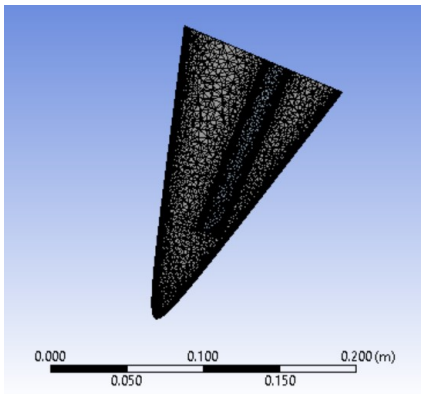

(b) Mesh for $\phi = 30, L_1/D = 6 \& L/D = 4.25$

Fig. 9: Experimental Data vs Computational data for Surface Nusselt Number

The geometrical setup is shown in figure above. The boundary topmost inner circular portion is free stream inlet of flow. The wall had uniform heat flux of $6000 W/m^2$. The inlet temperature of free stream is 300 K. The outlet condition is kept as Pressure outlet as in our problem whole configuration is enclosed by atmospheric pressure.

The meshing has been done to set greater nodes near wall compared to other regions. The figure above shows the same. The table below contains information about the parameters that had been varied to obtain the grid insensitive results. The student license has a limit of 512000 elements hence i had to stop after achieving a number near the threshold value.

Grid_ID	Inflation Layers(cone/pipe)	Face Sizing(m)	Number of Nodes	Number of Elements	Element Behaviour
Grid-1	20/20	0.0026	1,79,164	4,05,746	Linear
Grid-2	25/25	0.003	1,87,982	4,74,590	Linear
Grid-3	20/20	0.0023	2,21,038	5,02,389	Linear

TABLE III: Grid Info 1 30°for $\phi = 30, L_1/D = 6 \& L/D = 4.25$

Computational Results:
The surface Nusselt Number along conical wall plate at different angles had been computed from ANSYS for all three cases(see fig below). The convention of choosing angles has been shown according to the figure attached below. The grid 3 results had been chosen for comparison with experimental data provided. The plot below shows the comparison between experimental and computational results.

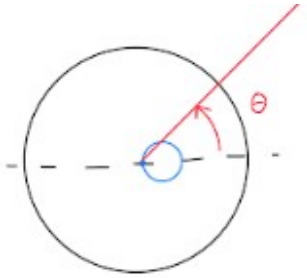

Fig. 10: Convention for angles

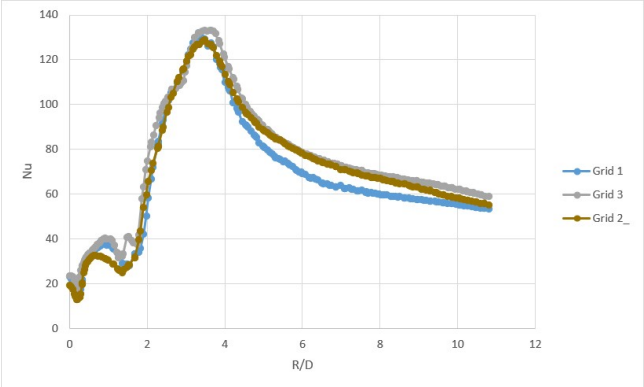

(a) Grid 1, 2 and 3 at $\theta = 0$

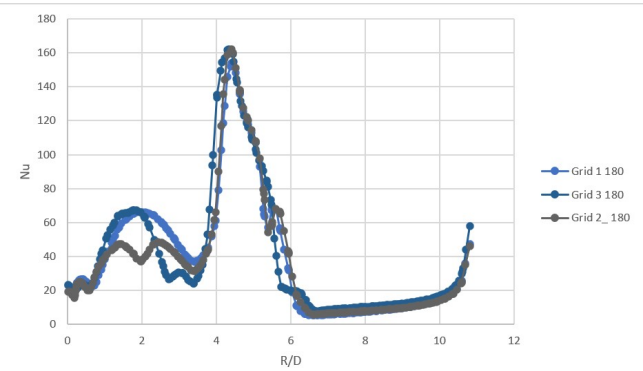

(b) Grid 1, 2 and 3 at $\theta = 180$

Fig. 11: Grid Insensitive Results

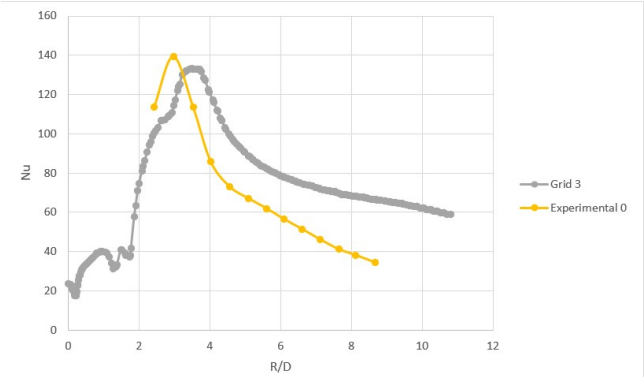

(a) Experimental Data vs Computational data at $\theta = 0$

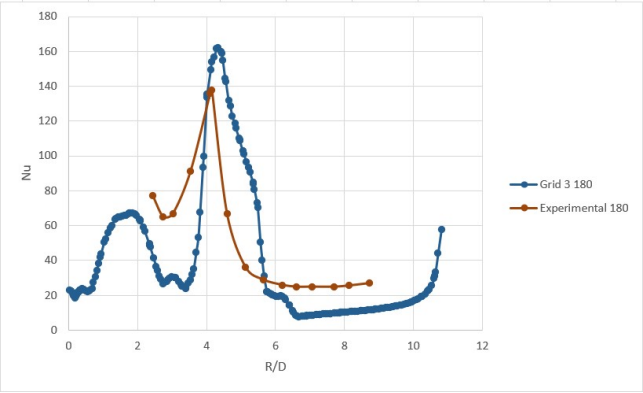

(b) Experimental Data vs Computational data at $\theta = 180$

Fig. 12: Experimental Data vs Computational data for Surface Nusselt Number

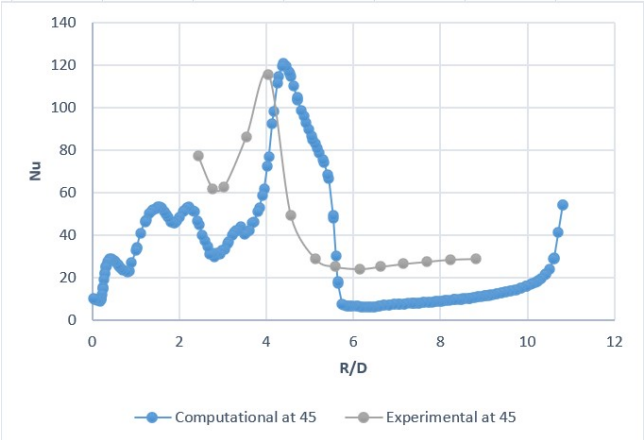

(a) Experimental Data vs Computational data at $\theta = 45$

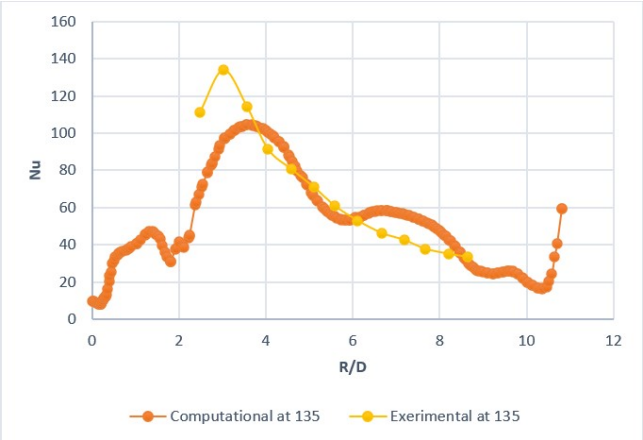

(b) Experimental Data vs Computational data at $\theta = 135$

Fig. 13: Experimental Data vs Computational data for Surface Nusselt Number

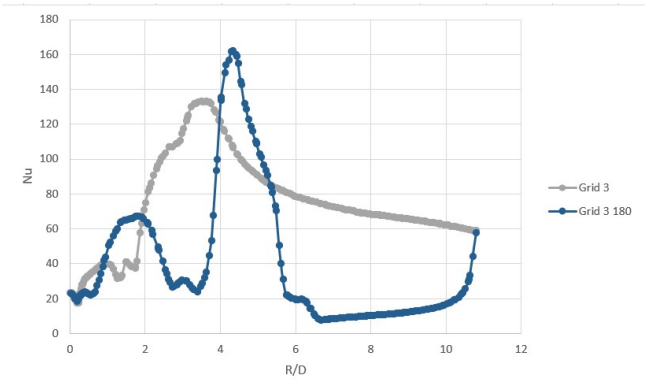

(a) Superimposed for $\theta = 0$, and $\theta = 180$

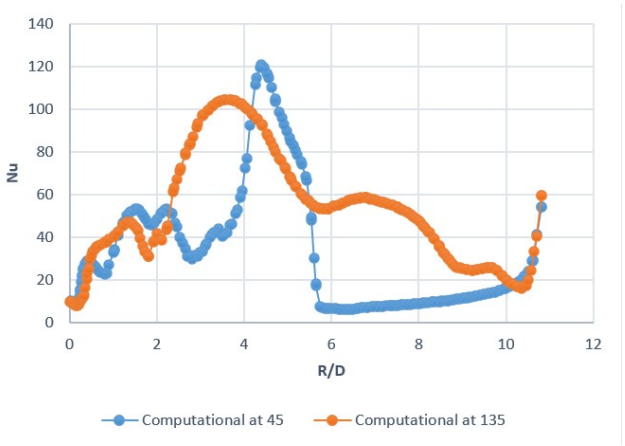

(b) Superimposed for $\theta = 45$, and $\theta = 135$

Fig. 14: Superimposed Plots

Conclusions:

- The maximum variation in Nusslet number($\theta = 0$) after R/D = 2 in plot between Grid 1 and Grid 2 is nearly 12%, while for Grid 2 and Grid 3 it's about 6.8%. Hence changing grid size further will not result in much significant change. We are interested in region after R/D = 2 as we have the experimental data in that region only due to experimental limitations.The error in region of $R/D > 7$ is much larger nearly 90%.
- The error in the position of peak of Nusselt number for $\theta = 0$ is about 17% while for $\theta = 180$ it is 3.9%. The error in the peak values of Nusselt number for $\theta = 0$ is about 14% while for $\theta = 180$ it is 5%. The general trend in Nusselt number obtained computationally is similar to the trend observed from experimental data.
- The velocity vector plot is shown below depicts how the flow pattern is over walls after jet crosses nozzle.

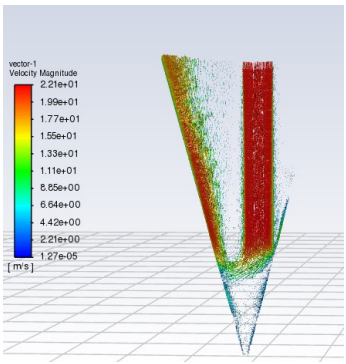

(a) Velocity Vectors

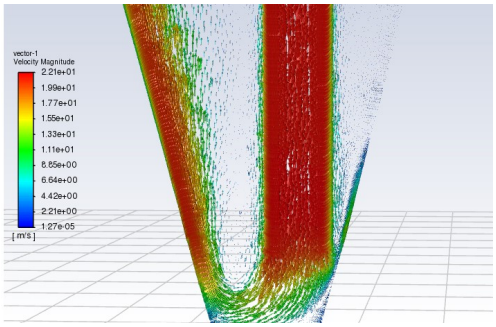

(b) Velocity Vectors Zoomed view

Fig. 15: Velocity Vectors

- The turbulence intensity and surface Nusselt number both have the maximum value around same region as we can see the contour attached below.

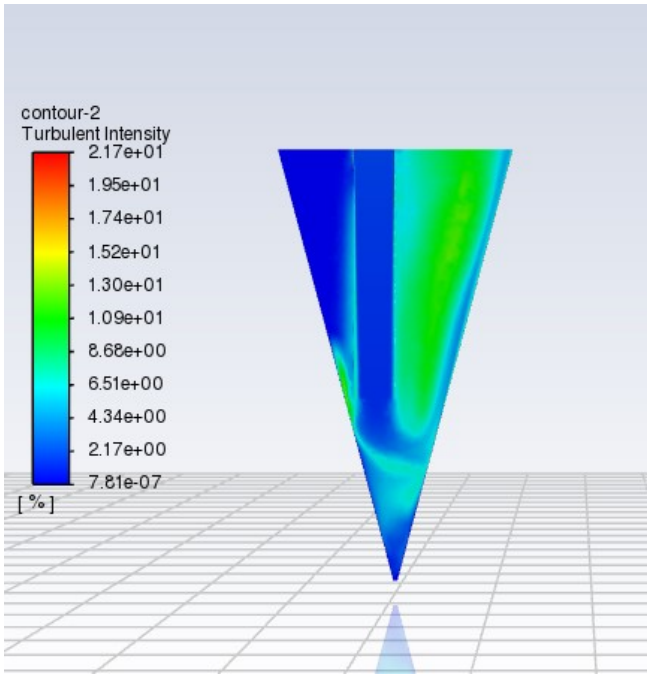

(a) Turbulence Intensity Contour

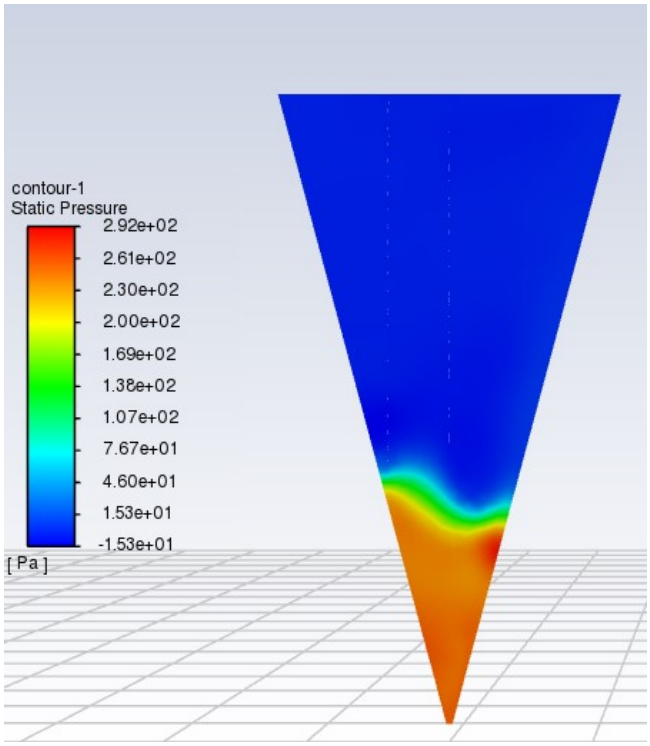

(b) Static Pressure Contour

Fig. 16: Contours

- The Pressure has a sharp declined as soon as it reaches the region of peak turbulence intensity.
- The plots have been superimposed and we have the shifted peak of the Nusselt number observed moving from $\theta = 0$ to $\theta = 180$ also for $\theta = 45$ to $\theta = 135$

- **(B)** $\phi = 70, Re = 82,000, L_1/D = 4 \& L/D = 3$ **::**

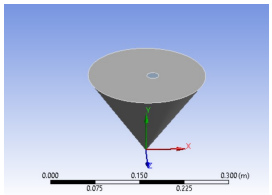

(a) Geometry for $\phi = 70, L_1/D = 4 \& L/D = 3$

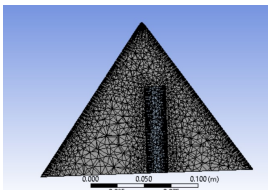

(b) Mesh for $\phi = 70, L_1/D = 4 \& L/D = 3$

Fig. 17: Experimental Data vs Computational data for Surface Nusselt Number

The geometrical setup is shown in figure above. The boundary topmost inner circular portion is free stream inlet of flow. The wall had uniform heat flux of $6000 W/m^2$. The inlet temperature of free stream is 300 K. The outlet condition is kept as Pressure outlet as in our problem whole configuration is enclosed by atmospheric pressure.

The meshing has been done to set greater nodes near wall compared to other regions. The figure above shows the same. The table below contains information about the parameters that had been varied to obtain the grid insensitive results.

Grid_ID	Inflation Layers(cone/pipe)	Face Sizing(m)	Number of Nodes	Number of Elements	Element Behaviour
Grid-1	35/25	0.004	9,34,359	3,95,628	Quadratic
Grid-2	28/25	0.0035	9,60,679	4,12,521	Quadratic

TABLE IV: Grid Info 1 30°for $\phi = 70, L_1/D = 4 \& L/D = 3$

Computational Results:

The surface Nusselt Number along conical wall plate at different angles had been computed from ANSYS for both the cases(see fig below). The grid 2 results had been chosen for comparison with experimental data provided. The plot below shows the comparison between experimental and computational results.

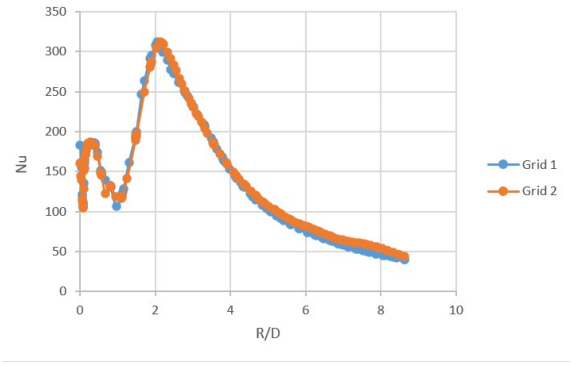

(a) Grid 1 and 2 at $\theta = 0$

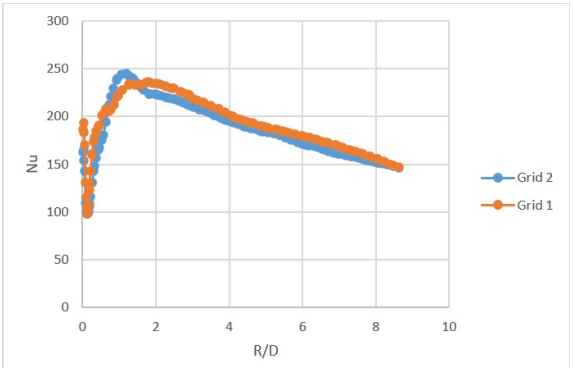

(b) Grid 1 and 2 at $\theta = 180$

Fig. 18: Grid Insensitive Results

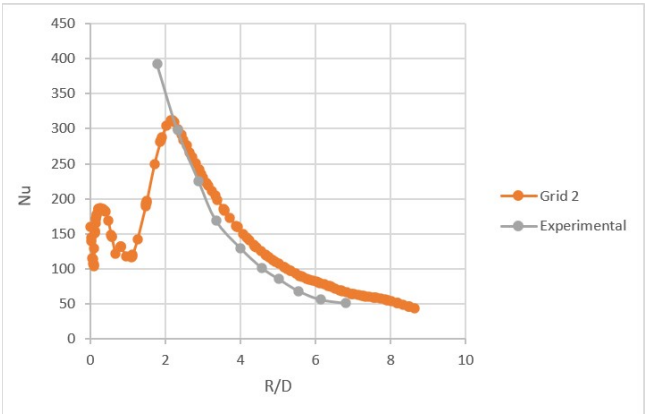

(a) Experimental Data vs Computational data at $\theta = 0$

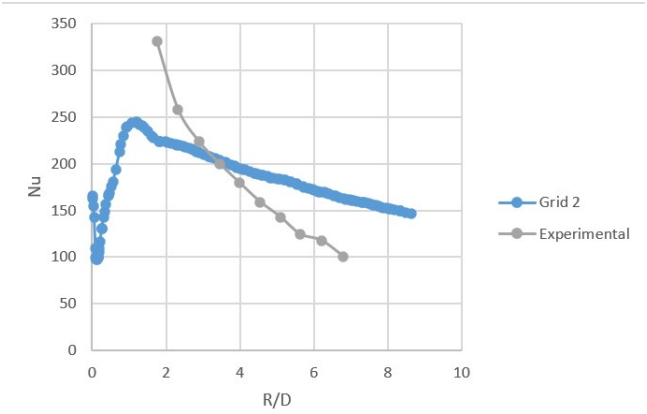

(b) Experimental Data vs Computational data at $\theta = 180$

Fig. 19: Experimental Data vs Computational data for Surface Nusselt Number

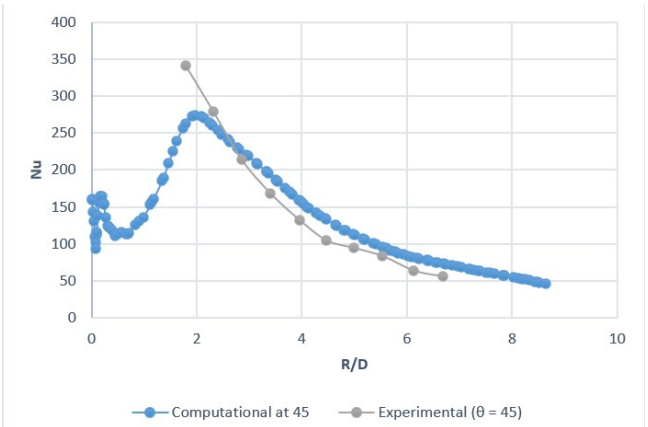

(a) Experimental Data vs Computational data at $\theta = 45$

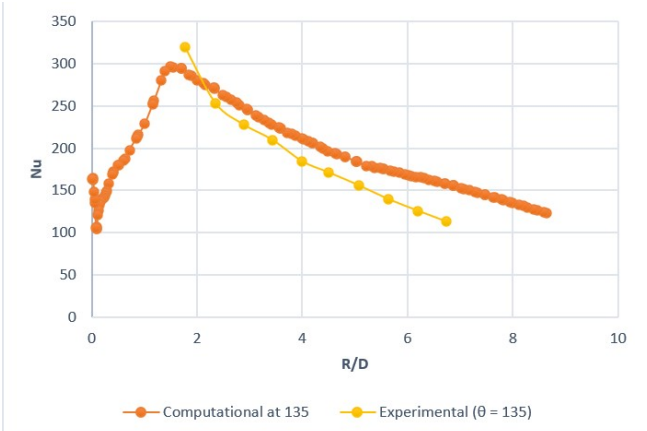

(b) Experimental Data vs Computational data at $\theta = 135$

Fig. 20: Experimental Data vs Computational data for Surface Nusselt Number

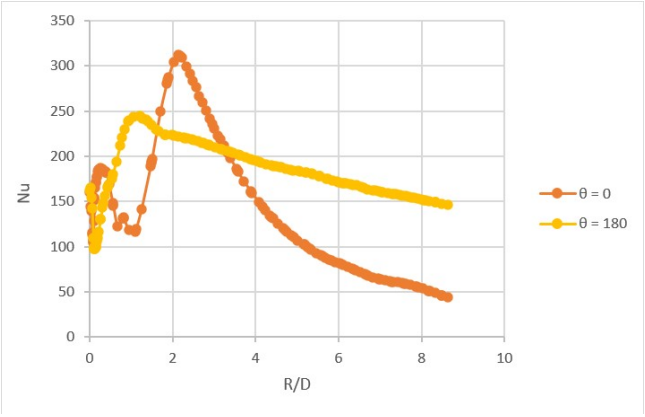

(a) Superimposed for $\theta = 0$, and $\theta = 180$

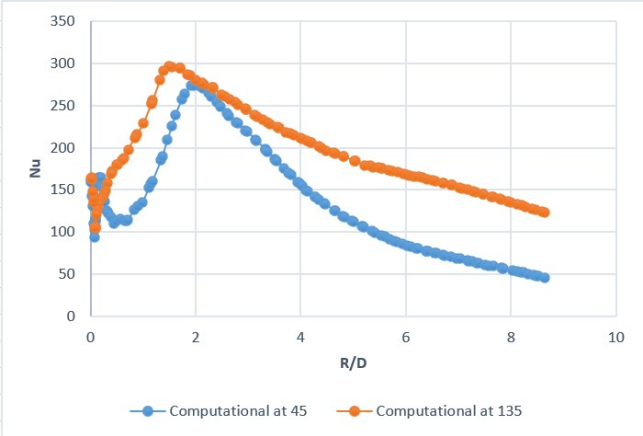

(b) Superimposed for $\theta = 45$, and $\theta = 135$

Fig. 21: Superimposed Plots

Conclusions:

- The maximum variation in Nusslet number($\theta = 0$) after R/D = 1.8 in plot between Grid 1 and Grid 2 is less than 5% and for $\theta = 180$ after R/D = 1.8 is 6.5%. Hence changing grid size further will not result in much significant change. We are interested in region after R/D = 1.8 as we have the experimental data in that region only due to experimental limitations.
- The maximum error in the values of Nusselt number for $\theta = 0$ is about 37% while for $\theta = 180$ it is 58% in region $R/D > 6$. The maximum error in the values of Nusselt number for $\theta = 45$ is about 30% while for $\theta = 135$ it is 38% in region $R/D > 6$.
- The velocity vector plot is shown below depicts how the flow pattern is over walls after jet crosses nozzle.

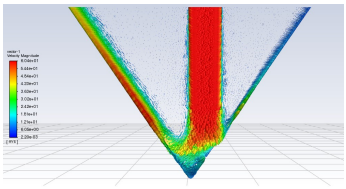

(a) Velocity Vectors

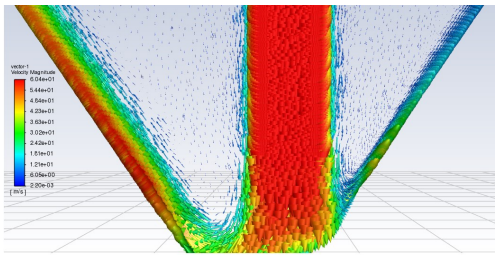

(b) Velocity Vectors Zoomed view

Fig. 22: Velocity Vectors

- The turbulence intensity and surface Nusselt number both have the maximum value around same region as we can see the contour attached below.

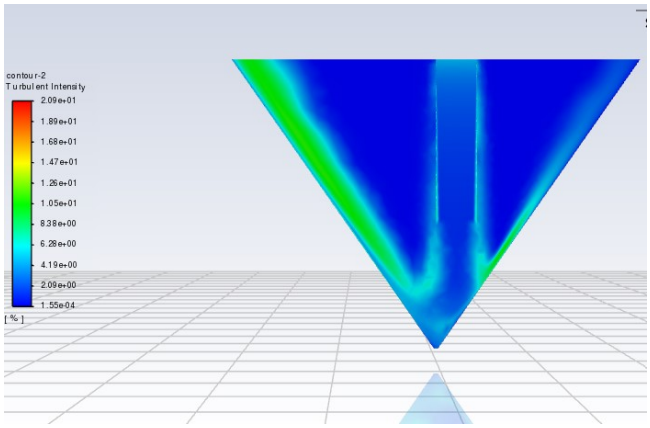

(a) Turbulence Intensity Contour

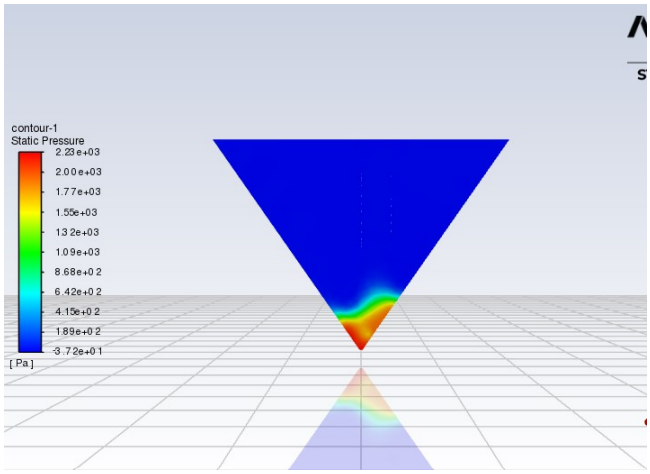

(b) Static Pressure Contour

Fig. 23: Contours

- The Pressure has a sharp declined as soon as it reaches the region of peak turbulence intensity.
- The plots have been superimposed and we have the shifted peak of the Nusselt number observed moving from $\theta = 0$ to $\theta = 180$ also for $\theta = 45$ to $\theta = 135$

- **(C)** $\phi = 30, Re = 29,000, L_1/D = 0 \& L/D = 10.25$ **::**

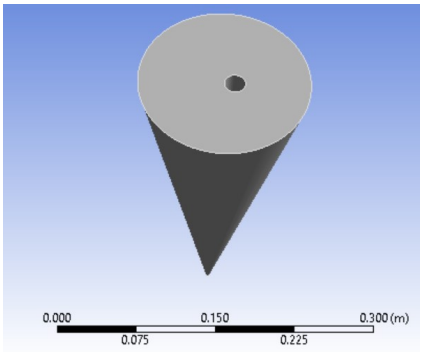

(a) Geometry for $\phi = 30, L_1/D = 0 \& L/D = 10.25$

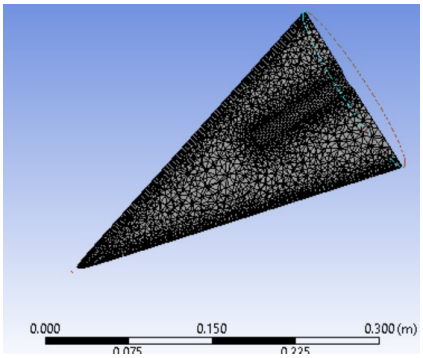

(b) Mesh for $\phi = 30, L_1/D = 0 \& L/D = 10.25$

Fig. 24: Experimental Data vs Computational data for Surface Nusselt Number

The geometrical setup is shown in figure above. The free stream inlet of flow is given on the circular cross-section inside the conical structure with cylindrical cavity in it.. The wall had uniform heat flux of $6000 W/m^2$. The inlet temperature of free stream is 300 K. The outlet condition is kept as Pressure outlet as in our problem whole configuration is enclosed by atmospheric pressure.

The meshing has been done to set greater nodes near wall compared to other regions. The figure above shows the same.

Inflation Layers	Face Sizing(m)	Number of Nodes	Number of Elements	Element Behaviour
25	0.004	9,48,131	4,13,199	Quadratic

TABLE V: Grid Info 1 30°for $\phi = 30, L_1/D = 0 \& L/D = 10.25$

Computational Results:
The surface Nusselt Number along conical wall plate at different angles had been computed from ANSYS(see fig below).

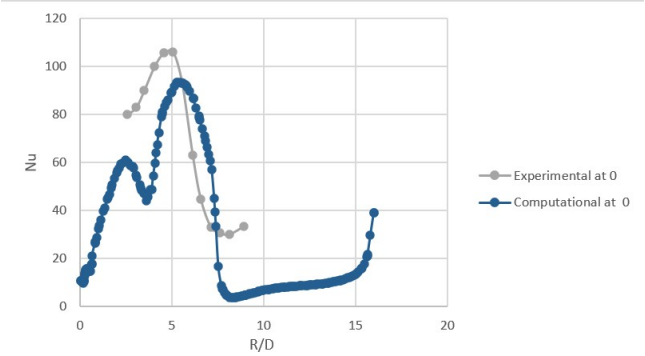

(a) Experimental Data vs Computational data at $\theta = 0$

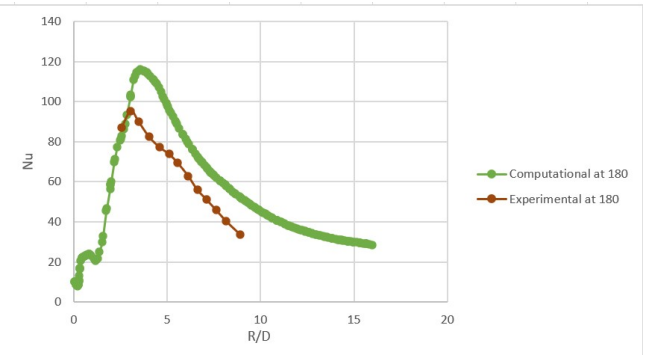

(b) Experimental Data vs Computational data at $\theta = 180$

Fig. 25: Experimental Data vs Computational data for Surface Nusselt Number

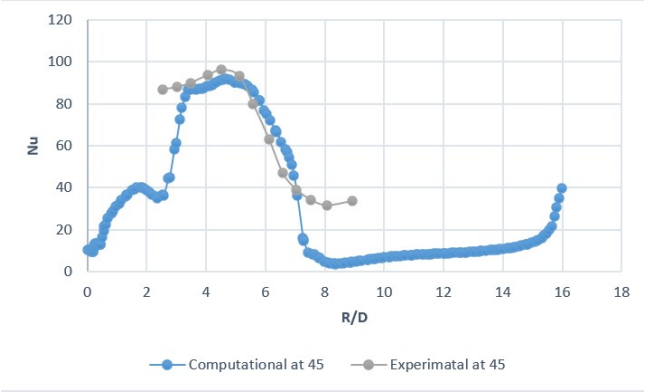

(a) Experimental Data vs Computational data at $\theta = 45$

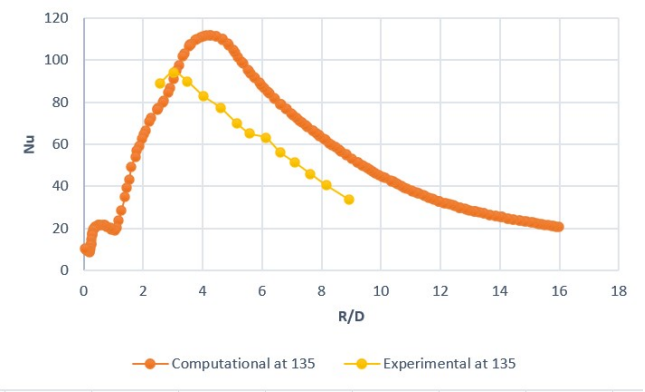

(b) Experimental Data vs Computational data at $\theta = 135$

Fig. 26: Experimental Data vs Computational data for Surface Nusselt Number

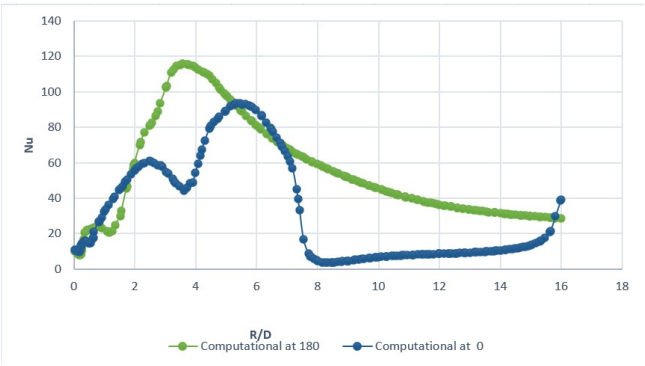

(a) Superimposed for $\theta = 0$, and $\theta = 180$

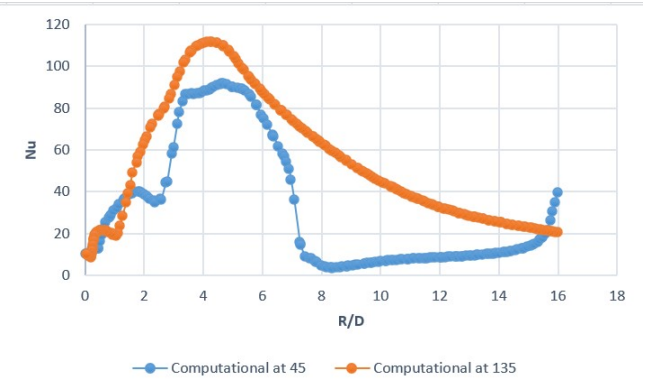

(b) Superimposed for $\theta = 45$, and $\theta = 135$

Fig. 27: Superimposed Plots

Conclusions:

- We are interested in region after R/D = 2 as we have the experimental data in that region only due to experimental limitations.
- The error between position of experimental peak and computationally obtained peak for $\theta = 0$ is 7.5% and for $\theta = 180$ is 16.3%
- The maximum error in the values of Nusselt number for $\theta = 0$ is about 48% while for $\theta = 180$ it is 58% in region $R/D > 6$.
- The velocity vector plot is shown below depicts how the flow pattern is over walls after jet crosses nozzle.

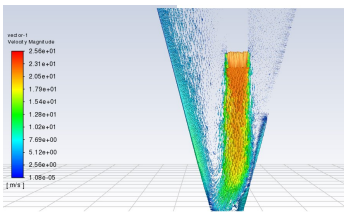

(a) Velocity Vectors

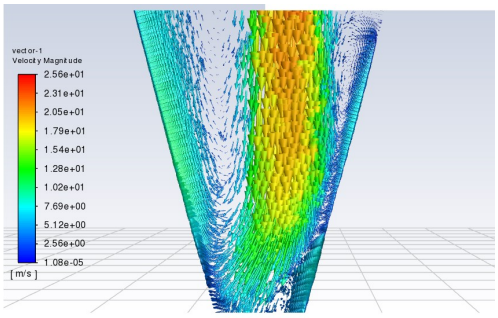

(b) Velocity Vectors Zoomed view

Fig. 28: Velocity Vectors

– The turbulence intensity and surface Nusselt number both have the maximum value around same region as we can see the contour attached below.

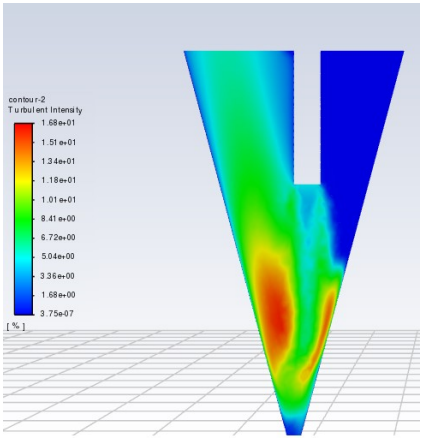

(a) Turbulence Intensity Contour

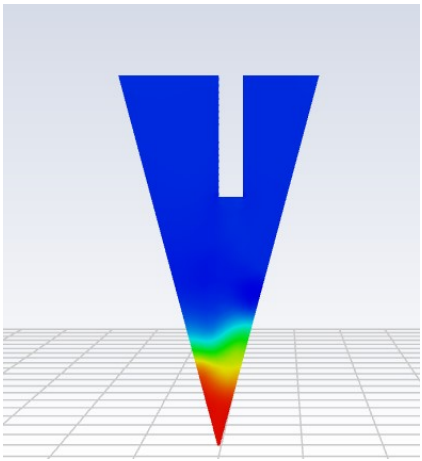

(b) Static Pressure Contour

Fig. 29: Contours

– The Pressure has a sharp declined as soon as it reaches the region of peak turbulence intensity.
– The plots have been superimposed and we have the shifted peak of the Nusselt number observed moving from $\theta = 0$ to $\theta = 180$ also for $\theta = 45$ to $\theta = 135$

IV. RESHAPING THE APEX OF CONE TO HEMISPHERE

- **(A)** $\phi = 30, Re = 29,000, L_1/D = 6.25, L/D = 4.25 \& D_1/D = 1$ **::**

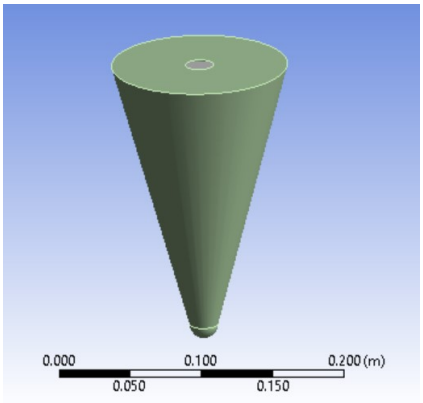

(a) Geometry

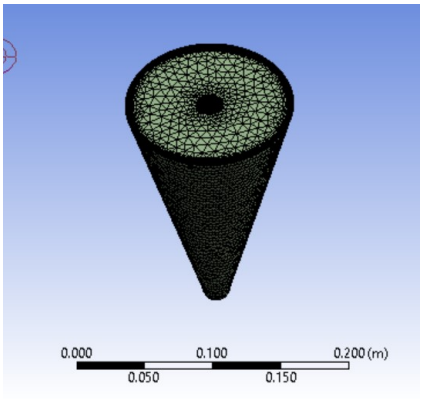

(b) Mesh

Fig. 30: Geometry and Mesh

The geometrical setup is shown in figure above. The boundary topmost inner circular portion is free stream inlet of flow. The wall had uniform heat flux of $6000W/m^2$. The inlet temperature of free stream is 300 K. The outlet condition is kept as Pressure outlet as in our problem whole configuration is enclosed by atmospheric pressure. The apex region has been replaced by an hemispherical end with Diameter of 0.02m.

Edge Divisions	Inflation Layers	Face Sizing(m)	Number of Nodes	Number of Elements	Element Behaviour
80	25	0.005	9,07,615	2,91,166	Quadratic

TABLE VI: Grid Info

- **(B)** $\phi = 30, Re = 29,000, L_1/D = 6.25, L/D = 4.25 \& D_1/D = 2.0541$ **::**

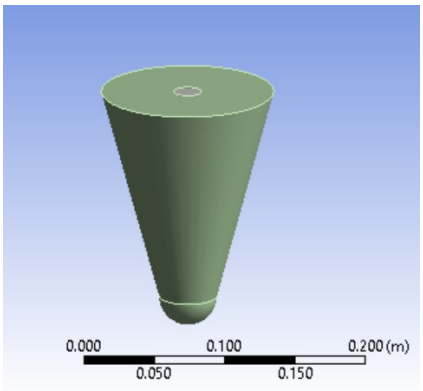

(a) Geometry

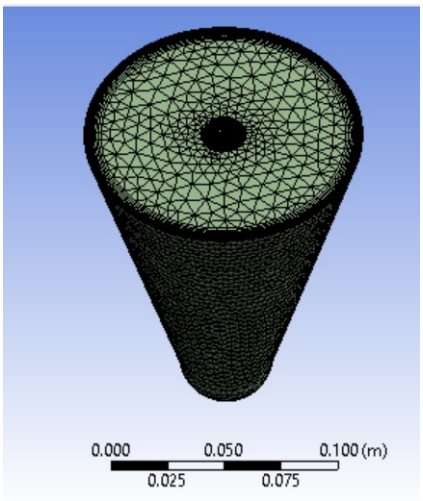

(b) Mesh

Fig. 31: Geometry and Mesh

The geometrical setup is shown in figure above. The boundary topmost inner circular portion is free stream inlet of flow. The wall had uniform heat flux of $6000W/m^2$. The inlet temperature of free stream is 300 K. The outlet condition is kept as Pressure outlet as in our problem whole configuration is enclosed by atmospheric pressure. The apex region has been replaced by an hemispherical end with Diameter of 0.041082 m.

Edge Divisions	Inflation Layers	Face Sizing(m)	Number of Nodes	Number of Elements	Element Behaviour
80	25	0.005	8,93,901	2,85,365	Quadratic

TABLE VII: Grid Info

Computational Results:
The surface Nusselt Number along conical wall plate at different angles had been computed from ANSYS. The convergence criteria used for all the parameters were 10^{-3} except for energy which had 10^{-6}. The computations had been stopped when the residuals reached the order of these criteria.

Conclusions:

- The plot of Nusselt number for Blend of diameter = 0.02 m diameter = 0.041082 and with apex have been attached below.

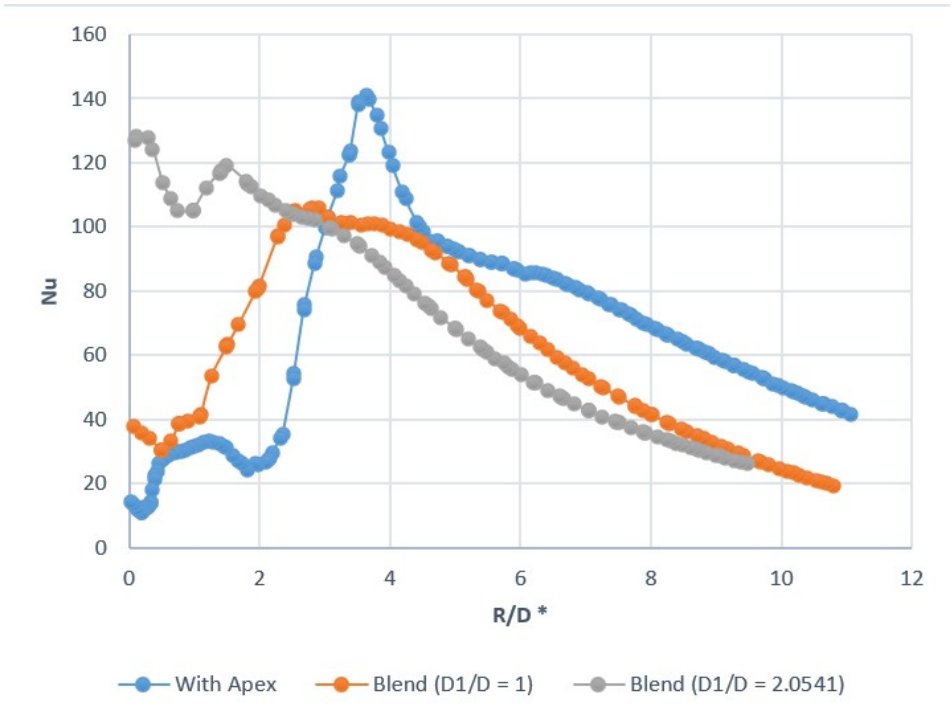

Fig. 32: Nusselt Number Plot at various Blend Radii
**See Apendix B for R/D convention for blended geometry*

- The peak of Nusslet Number has shifted leftwards as we have blended the end, while the Nusselt number has increased in the region $R/D < 4$.
- For the case with $D_1/D = 2.0541$ the Nusselt peak can be seen at $R/D \approx 0$

APPENDIX A
TERMINOLOGY

- The parameters L_1, L and ϕ are as in the figure:

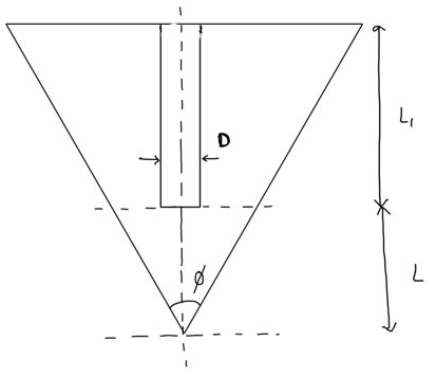

Fig. 33: Figure

- **Eccentricity:** The cone axis-to-impinged-cylindrical-jet-axis spacing(O) ratio to the nozzle diameter(D)[Fig : XX]

(a) Front View

(b) Top View

Fig. 34: Eccentricity Definition

- **Outlet Conditions:**
  - ***Pressure Outlet:*** In this condition we specify the gauge pressure at the outlet face. The flow at exit is monitored with some specified pressure, the flow may or may not achieve the fully developed state at exit. The diffusion flux for the flow variables in this case can be no-zero.

  - ***Outflow:***Outflow condition assumes a zero diffusion flux for all flow variables. Physically it is consistent with a fully-developed flow assumption, when there is no area change at the outflow boundary. In this, only the diffusion fluxes in the direction normal to the exit plane are assumed to be zero.

APPENDIX B
BLENDED GEOMETRY

- For the curved part the length along the hemishphere would be added(as part of R in R/D expression) and then the straight part inclined at angle 75°from x axis.

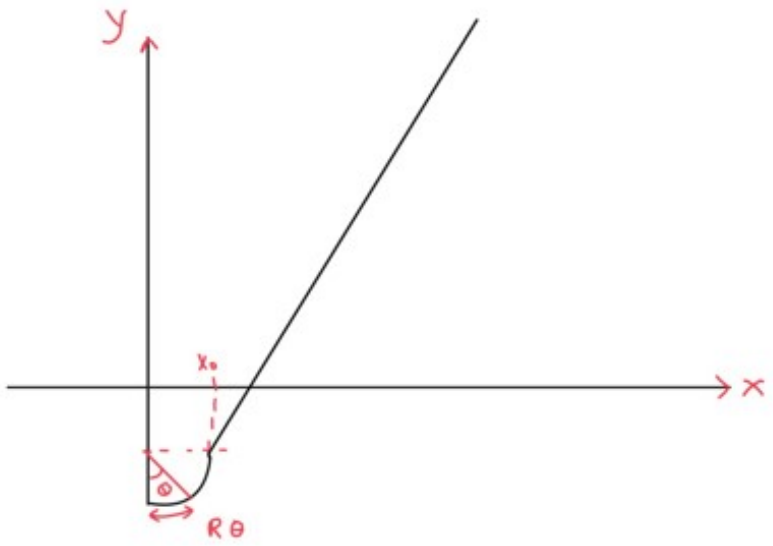

Fig. 35: Figure